Cocrystallization and Phase Segregation of Polyethylene Blends between the D and H Species. 8. Small-Angle Neutron Scattering Study of the Molten State and the Structural Relationship of Chains between the Melt and the Crystalline State

Kohji Tashiro,*,† Kouji Imanishi,† Masaaki Izuchi,† Masamichi Kobayashi,† Yuji Itoh,‡ Masayuki Imai,‡ Yasuo Yamaguchi,§ Masayoshi Ohashi,§ and Richard S. Stein‖

Department of Macromolecular Science, Faculty of Science, Osaka University, Toyonaka, Osaka 560, Japan; Institute for Solid State Physics, The University of Tokyo, Roppongi, Tokyo 106, Japan; Institute for Materials Research, Tohoku University, Sendai, Miyagi 980, Japan; and Polymer Research Institute, University of Massachusetts, Amherst, Massachusetts 01003

Received March 28, 1995; Revised Manuscript Received September 5, 1995⊗

ABSTRACT: Small-angle neutron scatterings have been measured for the molten state and the crystalline state of polyethylene (PE) blends between the fully deuterated high-density PE (DHDPE) and the hydrogeneous PE with various degrees of branching. Quantitative analysis based on the random-phase approximation has clarified that for both the blend samples of DHDPE/LLDPE(2) and DHDPE/LLDPE-(3) the D and H chains are miscible in the molten state, where LLDPE(2) is a linear low-density PE with ca. 17 ethyl branchings/1000 carbon atoms and LLDPE(3) is that with ca. 41 branchings. This result allows us to speculate that the difference in the crystallization behavior between the DHDPE/LLDPE(2) blend (cocrystallization) and DHDPE/LLDPE(3) blend (phase segregation) is not determined by the chain aggregation state in the melt but is governed more significantly by the kinetic effect during the crystallization process from the melt, as already pointed out on the basis of the time-resolved small-angle X-ray scattering and infrared spectral measurements. The radius of gyration (R_g) of the chain has been evaluated from the SANS data for the molten state as well as for the crystalline state. Even for the samples crystallized slowly from the melt, the R_g was found to be nearly equal to that of the crystalline state, supporting the random-reentry-type chain folding model for the crystalline lamellae of the cocrystallized DHDPE/LLDPE(2) blend sample.

Introduction

In a series of papers[1−7] we have investigated the crystallization behavior of polyethylene (PE) blends on the basis of X-ray diffraction, FTIR, DSC, and so on. These blends consisted of the fully deuterated high-density PE (DHDPE) and the hydrogeneous or normal PE with various degrees of ethyl branching. Utilization of the D species was originally aimed at observing the crystallization behavior of the individual components of the blends separately and from the molecular level. The crystallization of the blends between the D and H species has been found to change sensitively depending on the degree of branching of the H species. For example, in the DHDPE/LLDPE(2) blend system, where LLDPE(2) is a linear low-density PE with ca. 17 ethyl branching/1000 carbon atoms, the H and D chains cocrystallize; i.e., they are packed together in a common lamella *even when the sample is crystallized by slow cooling from the melt.* On the contrary, for the blends of DHDPE with LLDPE(3) of higher degree of branching (ca. 41) or with the high-density PE (HDPE) having no branching, the H and D chains crystallize basically in separated lamellar crystals. Of course, these descriptions are only approximate and the degree of cocrystallization and phase segregation changes sensitively by changing the D/H blend content and/or the sample history.

In previous papers,[6,7] we clarified an intimate relationship between the degree of cocrystallization and the crystallization rate. That is, DHDPE and LLDPE(2) show relatively similar crystallization rates in the isothermal crystallization process from the melt. On the other hand, the crystallization of HDPE is much faster and that of LLDPE(3) is much slower than that of DHDPE and this large difference in crystallization rates may relate with the phase segregation phenomenon between the D and H species. Of course we cannot ignore the thermodynamic stability of the blend: even when the crystallization rates are close to each other, the two species may segregate if they are not thermodynamically intimate. At this stage we may have questions: at what stage and with what mechanism are such phenomena induced? In the case of phase segregation, for example, we may speculate the following. (i) The H and D components are mixed homogeneously in the melt. As the temperature approaches the crystallization point, the H and D chains migrate at different diffusion rates to form clusters of their own species. Or (ii) the H and D chains are originally separated from each other in the melt and crystallize into the separated clusters. In order to check the reasonableness of these hypotheses, it may be necessary to clarify the aggregation states of the H and D chains in the melt. In this paper, we will study the miscibility of the D and H species in the molten state for the various D/H blends based on small-angle neutron scattering (SANS) experiments, which utilizes the difference in neutron scatter-

† Osaka University.
‡ The University of Tokyo.
§ Tohoku University.
‖ University of Massachusetts.
⊗ Abstract published in *Advance ACS Abstracts,* November 1, 1995.

0024-9297/95/2228-8484$09.00/0

ing length between the H and D atoms, and discuss the relationship between the miscibility and the degree of branching. The SANS experiment is also useful to investigate the statistical distribution of the H and D chains in the solid state,[8] which may be associated with the IR data analysis. In particular, the distribution of the H and D chain stems in the crystalline lattice is also important in relation to the chain-folding problem. In the latter half of this paper, the data of the wide-angle and small-angle neutron scatterings measured at room temperature will be also included in the discussion.

Experimental Section

Samples. The samples used in the high-temperature SANS measurements were DHDPE, LLDPE(2), and LLDPE(3) with the following characteristics.

	M_w	M_n	ethyl branching/1000 C
DHDPE	80 000	14 000	2–3
LLDPE(2)	75 000	37 000	17
LLDPE(3)	61 000	20 000	41

Both the blends of DHDPE/LLDPE(2) and DHDPE/LLDPE-(3) have the D/H composition of 50/50 wt %. These samples were prepared with the same method described in previous papers.[1-7] The samples were melted and pressed on the hot plate to form a disk with 1 mm thickness. In order to remove voids, the samples were kept at 160 °C in a vacuum oven for 3 h and then cooled slowly to room temperature.

SANS Measurements. SANS measurements were performed by using a SANS-U system of the Institute for Solid State Physics, the University of Tokyo, which is installed at the Tokai Research Establishment, Japan Atomic Energy Research Institute, Ibaraki, Japan. The sample-to-detector distance was 4 m, and the scattering signals were detected with a two-dimensional position sensitive detector. The wavelength (λ) was 7.0 Å. The available q range was $0.008 < q < 0.08$ Å^{-1}, where $q = (4\pi/\lambda)\sin(\theta/2)$ and θ is a scattering angle. The disk sample was sandwiched in a pair of quartz plates with a rubber spacer and set into the heater, which was installed into the sample chamber evacuated by a rotary pump. The sample temperature was monitored with a platinum resistance sensor. SANS was measured stepwise in the cooling process from the melt (ca. 190 °C) to ca. 100 °C.

All the scattering intensities were circularly averaged to give the scattering pattern as a function of q. The net scattering intensity of the sample, I_{sample}, was obtained by subtracting the scattering of the empty cell (I_{cell}) from the observed scattering (I_{obs}) after correction for the transmission ($\%T$).

$$I_{sample} = I_{obs} - (\%T_{sample}/\%T_{cell})I_{cell} \quad (1)$$

The conversion to the absolute scattering cross section $(d\Sigma/d\Omega)_{total}$ was carried out by using a data of lupolen (low-density PE) as a standard material:

$$\left(\frac{d\Sigma}{d\Omega}\right)_{total} = \left(\frac{d\Sigma}{d\Omega}\right)_{lupolen} \frac{I_{sample}}{I_{lupolen}} \frac{\%T_{lupolen}}{\%T_{sample}} \frac{d_{lupolen}}{d_{sample}} \quad (2)$$

where $\%T$ and d are the transmission and the thickness of the sample, respectively. The coherent cross section $(d\Sigma/d\Omega)_{coh}$ was obtained by subtracting the incoherent contribution of the H species:

$$\left(\frac{d\Sigma}{d\Omega}\right)_{coh} = \left(\frac{d\Sigma}{d\Omega}\right)_{total} - \phi_H \frac{\rho_H}{\rho_{LLDPE(2)}} \left(\frac{d\Sigma}{d\Omega}\right)_{inc} \quad (3)$$

where the cross section of the pure LLDPE(2) sample was used as incoherent scattering data for the H component in the blend. ϕ_H is the volume fraction of the H component and ρ is a density. The volume of one monomeric unit was assumed to be the same for the H and D species, because the concentration of the side chains is not very high. $(d\Sigma/d\Omega)_{coh}$ is a function of temperature. The temperature dependence of ρ was calculated by using the volume 32.75 cm^3/mol of C_2H_4 units, which was calculated from the amorphous density of PE at room temperature, and the thermal expansion coefficient 7.5×10^{-4} K^{-1} above 110 °C.[9]

SANS Data Analysis. Structure factor $S(q)$ was calculated by the following equation

$$S(q) = \left(\frac{d\Sigma}{d\Omega}\right)_{coh} / [v^{-2}(b_H - b_D)^2] \quad (4)$$

where b_H and b_D are the scattering lengths of the H and D atoms, -0.166×10^{-12} and 3.998×10^{-12} cm, respectively. v is the volume per one monomer. According to the random-phase approximation (RPA), the structure factor of the mixture of two components A and B in the single-phase state is represented by[10]

$$\frac{1}{S(q)} = \frac{1}{v_A\phi_A N_A P_A(u)} + \frac{1}{v_B\phi_B N_B P_B(u)} - \frac{2\chi}{v} \quad (5)$$

where ϕ_i and N_i is the volume fraction and the degree of polymerization of ith component, respectively. χ is a Flory–Huggins interaction parameter and $v = (v_A v_B)^{1/2}$. $P_i(u)$ is a normalized form factor of the ith component and represented by the Debye function for the monodispersed Gaussian chain:

$$P_i(u) = \frac{2}{u^2}[\exp(-u) - 1 + u] \quad (6)$$

where $u = q^2(R_g)_i^2$ and $(R_g)_i^2$ is the mean square radius of gyration. Since the DHDPE sample used in the SANS experiments has a relatively wide molecular weight distribution, the following treatment may be necessary. By assuming the polydispersity with Schultz–Zimm-type distribution, the structure factor for a mixture of polydispersed polymers is given as follows[11]

$$\frac{1}{S(q)} = \frac{1}{v_A\phi_A N^n{}_A g_A(x)} + \frac{1}{v_B\phi_B N^n{}_B g_B(x)} - \frac{2\chi}{v} \quad (7)$$

where $N^n{}_i$ is the number-average degree of polymerization and $v = (\phi_A/v_A + \phi_B/v_B)^{-1}$. $g_i(x)$ is

$$g_i(x) = \frac{2}{x^2}\left[x - 1 + \left(\frac{h_i}{h_i + x}\right)^{h_i}\right] \quad (8)$$

where $x = q^2 (R_g{}^n)_i^2$ and $(R_g{}^n)_i$ is a number-average radius of gyration and h_i is defined by

$$h_i = \left[\frac{N^w{}_i}{N^n{}_i} - 1\right]^{-1} \quad (9)$$

For the q range of $q \ll R_g{}^n$, eq 7 is reduced to the so-called Ornstein–Zernike form:

$$\frac{1}{S(q)} = \frac{1}{S(0)}[1 + \xi^2 q^2] \quad (10)$$

$$\frac{1}{S(0)} = \frac{1}{v_A\phi_A N^w{}_A} + \frac{1}{v_B\phi_B N^w{}_B} - \frac{2\chi}{v} \quad (11)$$

where ξ denotes the correlation length. When $1/S(q)$ is plotted against q^2, $1/S(0)$ is obtained from an intercept and χ can be calculated by eq 11. In the actual analysis, plots of both eqs 7 and 10 were made and the obtained parameters were compared with each other to check the reasonableness of the data treatment.

Results and Discussion

DHDPE/LLDPE(2) Blend. Figures 1 and 2 show the $S(q)$ and the corresponding Kratky plot observed for

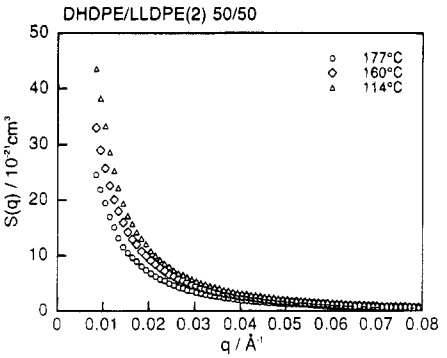

Figure 1. Temperature dependence of the structure factor $S(q)$ measured for the DHDPE/LLDPE(2) blend sample with D/H = 50/50 wt %.

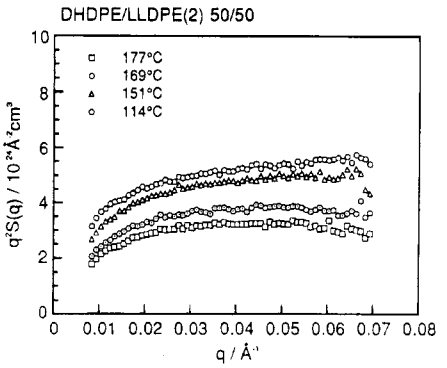

Figure 2. Temperature dependence of Kratky plot of $S(q)$ measured for the DHDPE/LLDPE(2) blend sample.

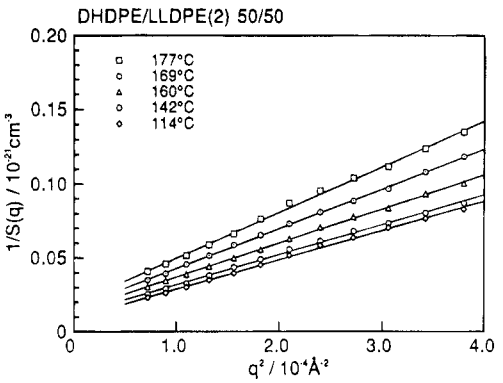

Figure 3. Temperature dependence of Gunier plot for DHDPE/LLDPE(2) blend sample.

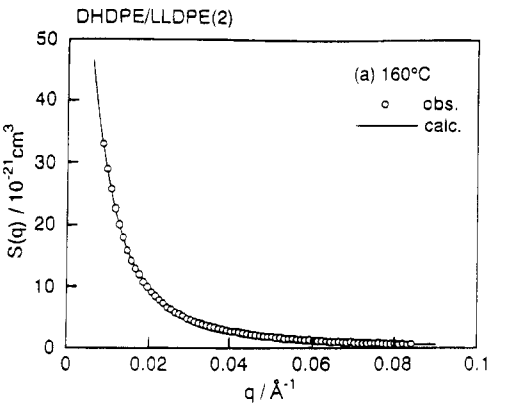

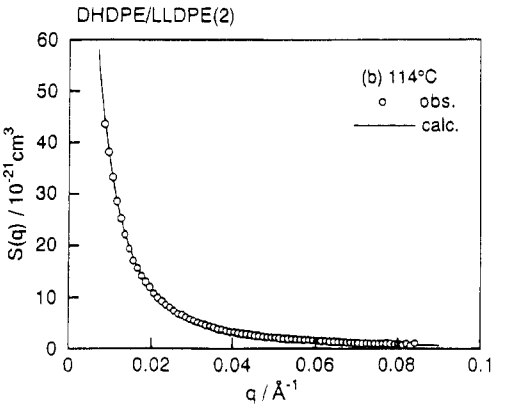

Figure 4. Illustration of curve fitting of $S(q)$ based on the RPA equation for DHDPE/LLDPE(2) blend sample in the molten state.

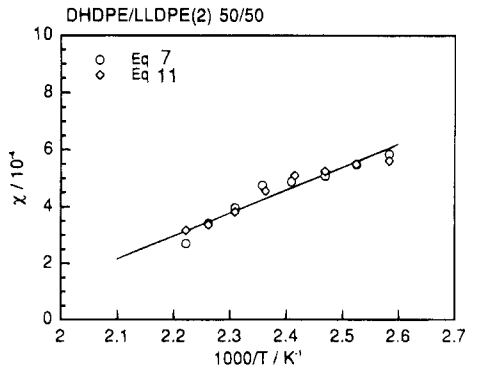

Figure 5. Temperature dependence of χ evaluated for DHDPE/LLDPE(2) blend sample by eqs 7 and 11 in the text.

the DHDPE/LLDPE(2) blend sample. In contrast to the data collected in the solid-state, no anomalous increase of the intensity was detected in Figure 2, indicating that the data can be interpreted reasonably based on the random coil chain statistics. Figure 3 shows the plot of $1/S(q)$ against q^2. At a range of $q < 0.025$ Å^{-1}, a good linear relationship can be seen. The curve fitting to the RPA equation (eq 7) is shown in Figure 4 as an example: both the curves observed at 160 and 114 °C could be reproduced well enough. A good fit to the RPA equation may indicate that the H and D components of this blend sample are mixed together in the melt, because originally the equation should be applied only to the single phase system. Figure 5 shows the interaction parameter χ estimated from eq 7. χ values evaluated by eq 11 are also shown in this figure. The χ values estimated by the different equations agree well with each other, indicating that the curve fitting in Figure 4, for example, is reasonable. The χ is approximately represented by the following equation as a function of temperature.

$$\chi = 0.80/T - 1.5 \times 10^{-3} \quad (12)$$

DHDPE/LLDPE(3) Blend. Figures 6 and 7 show, respectively, the $S(q)$ and the Kratky plots for the DHDPE/LLDPE(3) blend sample in the molten state. In contrast with the case of the DHDPE/LLDPE(2) blend sample, the $S(q)$ changes only slightly with temperature. Figure 8 shows the plot of $1/S(q)$ against q^2, giving a good linearity as likely as for the DHDPE/LLDPE(2) blend sample. The curve fit to the RPA is illustrated in Figure 9. In the case of the DHDPE/LLDPE(3) system, too, we may conclude that the D and H components are well mixed in the melt. The χ values obtained from eq 7 (and 11) are shown in Figure 10: The temperature dependence of the χ is represented by the following equation:

$$\chi = 0.82/T - 1.4 \times 10^{-3} \quad (13)$$

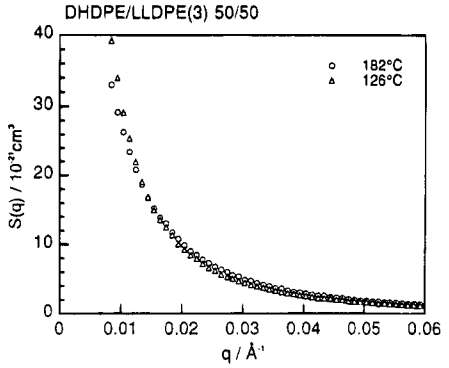

Figure 6. Temperature dependence of the structure factor $S(q)$ measured for the DHDPE/LLDPE(3) blend sample with D/H = 50/50 wt %.

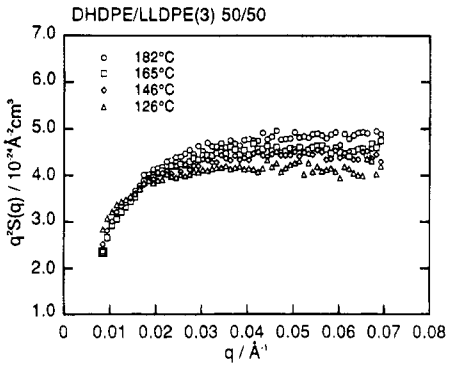

Figure 7. Temperature dependence of Kratky plot of $S(q)$ measured for the DHDPE/LLDPE(3) blend sample.

χ Values. The χ values reported by several authors through the SANS measurements made for the polyethylene D/H blend sample are $(3-6) \times 10^{-4}$ for the linear chain and $(7-16) \times 10^{-4}$ for the chain with a relatively high degree of branchings.[11-13] The χ values shown in Figure 10 are $(2-6) \times 10^{-4}$ for both the DHDPE/LLDPE(2) and DHDPE/LLDPE(3) samples, which are considered to be reasonable, judging from these values. These values are close to the χ value (ca. 4×10^{-4}) expected for the isotope effect on the linear chain, because the labeled chains are fully deuterated and the branch level of the LLDPE is low.[23-26]

According to the Flory–Huggins equation, the critical value of χ for the system with a finite distribution of molecular weight is written by[14-18]

$$\chi_c = \frac{1}{2}\left[\left(\frac{1}{(N^z_D/N^w_D)N^w_H}\right)^{1/2} + \left(\frac{1}{(N^z_H/N^w_H)N^w_D}\right)^{1/2}\right] \times \left[\left(\frac{(N^z_H/N^w_H)}{N^w_D}\right)^{1/2} + \left(\frac{(N^z_D/N^w_D)}{N^w_H}\right)^{1/2}\right] \quad (14)$$

where N^z_i is the z-average degree of polymerization and N^z_i/N^w_i can be rewritten as $N^z_i/N^w_i = (h_i + 2)/(h_i + 1)$. The calculated χ_c is 7.75×10^{-4} and 8.59×10^{-4} for the DHDPE/LLDPE(2) and the DHDPE/LLDPE(3) blend samples, respectively. As shown in Figure 10, the χ values for both of the blend samples do not reach the χ_c's in the whole region of the melt, suggesting that these blend systems do not show the phase segregation phenomenon at any temperature in the molten state. There have been presented two different conclusions for the mixing state of the branched and linear PEs: homogeneity[12,19] and phase segregation.[20-24] As long as we are only concerned about the PE blend samples

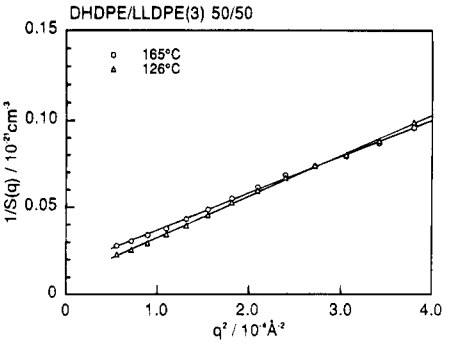

Figure 8. Temperature dependence of Gunier plot for DHDPE/LLDPE(3) blend sample.

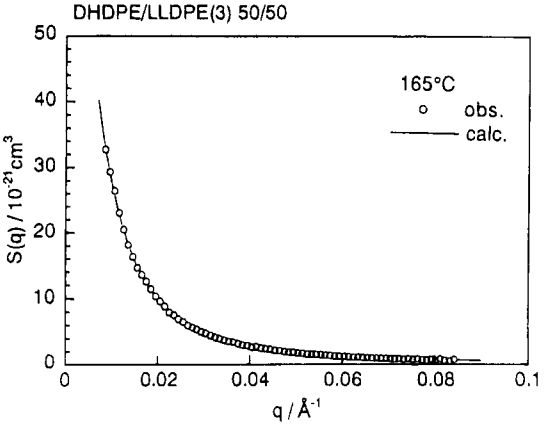

Figure 9. Illustration of curve fitting of $S(q)$ based on the RPA equation for DHDPE/LLDPE(3) blend sample in the molten state.

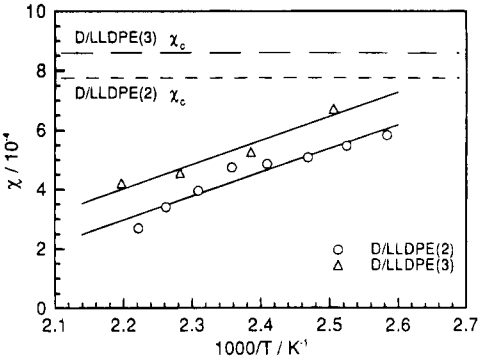

Figure 10. Comparison of χ between the DHDPE/LLDPE(2) and DHDPE/LLDPE(3) blend samples.

between DHDPE and hydrogeneous LLDPE, the linear and branched chains may be said to be mixed together homogeneously in the melt, as discussed in the present section.

Combining the SANS results with the crystallization kinetics data obtained by the SAXS[7] and FTIR[6] measurements, it may be considered that the difference in the crystallization behavior between the blends of DHDPE/LLDPE(2) and DHDPE/LLDPE(3) does not originate from the difference in the aggregation structure of the melt but the difference at the nucleation stage or the difference in the crystallization rates between the D and H chains is one of the most important factors. In the molten state, both the D and H chains are miscible with each other. Once the samples are cooled down below the crystallization temperature, the chains may diffuse more or less to form the cluster of the trans-zigzag chain stems. In the case of the DHDPE/LLDPE(2) blend, the D and H chains

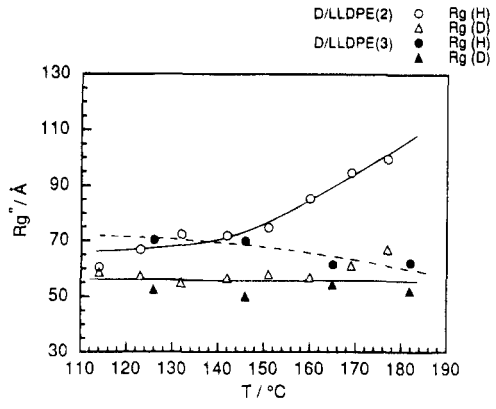

Figure 11. Temperature dependence of the number-averaged radius of gyration (R_g^n) obtained by the RPA equation: open circle, the H species of DHDPE/LLDPE(2) sample; open triangle, the D species of DHDPE/LLDPE(2) sample; solid circle, the H species of DHDPE/LLDPE(3) sample; and solid triangle, the D species of DHDPE/LLDPE(3) sample.

crystallize at almost the same rate,[6,7] so they do not separate but aggregate together into the same lamella and are stabilized energetically. On the other hand, in the case of the DHDPE/LLDPE(3) sample, the D chains migrate at a relatively high rate compared with the H chains with many side groups, resulting in the faster nucleation of the D lamella, with the H chains still remaining in the melt.

Radius of Gyration of the Molten Chains. Figure 11 shows the R_g^n of the H and D components in the melt evaluated from eq 7. It should be noticed that the R_g^n of the D component is almost the same for both the DHDPE/LLDPE(2) and DHDPE/LLDPE(3) blend samples; that is, the D chain in the melt shows almost the same spatial expansion independent of the branching content of the countercomponent. It is natural that the D chain dimensions are virtually independent of the other blend component as the branch content is negligibly small. However, a strong temperature dependence of the R_g^n is observed in the melt for the LLDPE(2) chain. When the temperature becomes closer to the crystallization point, ca. 110 °C, the R_g^n of LLDPE(2) changes gradually from the value of ca. 100 Å to 60 Å, which is almost coincident with the R_g^n of the D species. The R_g^n of LLDPE(3) is ca. 70 Å and does not change so much in this temperature region. The R_g^n of the Gaussian chain with effective segment length l is expressed by

$$(R_g^n)^2 = \frac{N^n l^2}{6} \tag{15}$$

The l value has been reported to be ca. 5.8 Å for the C_2H_4 unit.[25,26] Equation 15 gives the R_g^n values expected for the DHDPE, LLDPE(2), and LLDPE(3) chains as follows by assuming that the l value is not so different among these three types of chains because of the relatively low degree of ethyl branchings.

$$R_g^n = 50 \text{ Å for DHDPE}$$
$$86 \text{ Å for LLDPE(2)}$$
$$63 \text{ Å for LLDPE(3)}$$

These values correspond relatively well to the above-mentioned experimental values.

Comparison of R_g between Room Temperature and the Melt. Figure 12 shows the SANS profiles

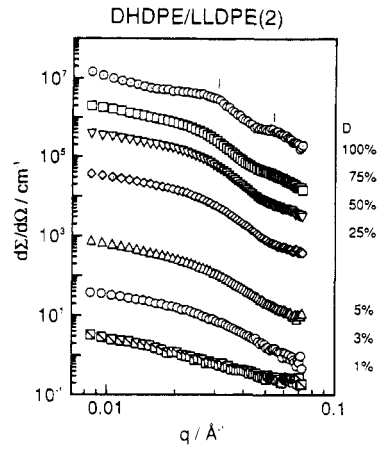

Figure 12. SANS profiles measured at room temperature for a series of DHDPE/LLDPE(2) blend samples.

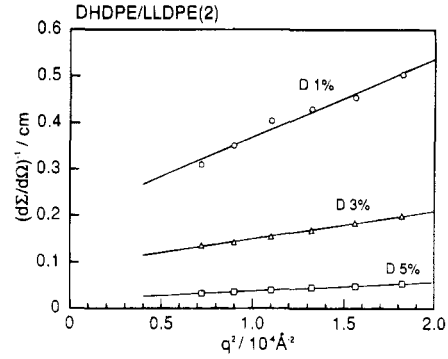

Figure 13. Plots of inversed SANS intensity against q^2 for DHDPE/LLDPE(2) blend samples with low D concentration.

measured at room temperature for a series of DHDPE/LLDPE(2) blend samples with different D/H composition, where some offset is added to each curve to avoid making the figure complex. The pure DHDPE sample shows the two peaks corresponding to the first- and second-order scatterings from the lamellar stacking with the long period of ca. 210 Å. By increasing the H content, these peaks are smeared gradually and the curves become broad. Figure 13 shows the Gunier plot for the samples with low concentration of the D species in the q range of 0−0.02 Å^{-1}. For the solid sample with diluted D component, the scattering intensity may be expressed as follows[27]

$$\frac{\phi_D(1-\phi_D)NK}{(d\Sigma/d\Omega)} = \frac{1}{N^w}\left[\left(1 - \frac{\phi_D \Delta w}{1+\Delta w}\right) + \frac{1}{3}(R_g^z)_D^2 q^2 \left(1 + \phi_D \frac{\Delta z - \Delta w}{1+\Delta w}\right)\right] \tag{16}$$

where N is the number of monomers per unit volume, and ϕ_D is a volume fraction of the D component. K is the scattering contrast and $K = (b_H - b_D)^2$. $(R_g^z)_D^2$ is the z-average mean square radius of gyration, and Δw and Δz are, respectively, the quantities related to the molecular weight difference between the H and D species:

$$N^w_H = N^w_D(1 + \Delta w)$$

$$N^z_H = N^z_D(1 + \Delta z)$$

The R_g^z obtained from eq 16 can be converted to the number-average value by a relation, $(R_g^n)_D^2 = (R_g^z)_D^2/$

Table 1. Parameters of DHDPE/LLDPE(2) Blend Evaluated at Room Temperature

D content/wt %	$N^{w}{}_{D}{}^{a}$	$N^{w}{}_{D}{}^{b}$	$(R_g{}^{n})_{D}{}^{b}$
1		1650	67
3		1218	58
5		3538	72
average	2500	2135	66

[a] Measured by GPC. [b] Estimated by SANS data (eq 16) where $(R_g{}^{n})_{D}{}^{2} = (R_g{}^{w})_{D}{}^{2}/(N^{w}{}_{D}/N^{n}{}_{D})$.

$(N^{z}{}_{D}/N^{n}{}_{D})$, where $N^{z}{}_{D}/N^{n}{}_{D} = (h_D + 2)/h_D$.[15,16] The $N^{w}{}_{D}$ and $(R_g{}^{n})_{D}$ estimated from Figure 13 are listed in Table 1. By comparing Table 1 with Figure 11, we may notice that the $(R_g{}^{n})_{D}$ measured at room temperature, ca. 66 Å on average, is nearly equal to that of the melt, ca. 60 Å. Ballard et al.[28] and Fischer et al.[29] found out the similar relation of R_g for the DHDPE/HDPE blend sample with highly diluted D content. But these samples were prepared by melt quenching in order to avoid a segregation (clustering) artifact between the H and D species. In contrast, our samples were prepared by slow cooling from the melt, and the segregation artifact was avoided by matching the crystallization rate of the two species, to produce an almost perfectly cocrystallized sample. In other words, we have for the first time confirmed the following important conclusion: the R_g is virtually the same in the molten and crystalline states and the overall distribution of mass elements in the chain (and hence the spatial geometry) is unaffected by the crystallization process.

Let us discuss here the crystallization mechanism of the cocrystallizable D/H blend system on the basis of all the experimental data obtained for the DHDPE/LLDPE(2) sample. As clarified by the above-mentioned SANS experiments, the D and H molecular chains are mixed homogeneously in the molten state. As the temperature is decreased below the crystallization point, the trans segments are generated in these random coils and form a cluster consisting of the crystalline stems, as already revealed by the time-resolved IR[6] and SAXS[7] measurements. The reservation of R_g on the way from the melt to the crystalline state may indicate that the spatial geometry of the whole chain is not modified so much during this regularization of structure. As to the chain folding structure, the random chain folding model may be applicable to the present DHDPE/LLDPE(2) blend, as supported by the infrared spectral data:[3,4] on the basis of the quantitative analysis of the infrared band splitting, we have pointed out that the band splitting width, which reflects sensitively the spatial arrangement of the D and H chain stems in the lamella, changes almost linearly with the D/H blend content. This means that the probability of positioning the D (or H) chains at a lattice site is almost proportional to the concentration of the D (or H) species. In other words, the chain stem arrangement is determined by the random statistics. Combining these two ideas, the similarity of the R_g in the melt and crystalline states and the random statistics of the stem arrangement, leads us to the model that the random coils regularize into the aggregation structure of the trans-zigzag chains keeping the entangled state of the D and H chains without a large change in the whole chain expansion. As a result this model may be similar to the "ersterrungsmodell (solidification model)" proposed by Fischer et al.,[30] in which the random coil chain is frozen into a solid with the averaged radius of gyration kept unchanged. But we should not confuse our model with theirs, because our model is for the almost perfectly cocrystallized D/H blend system which is obtained by slow cooling from the melt, quite different from the quenched sample used by them.

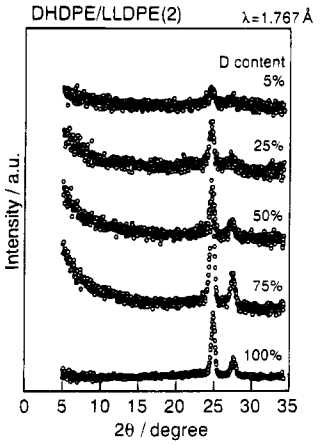

Figure 14. Composition dependence of the WANS data measured at room temperature for DHDPE/LLDPE(2) blend sample.

This consideration is supported also by the WANS data measured at room temperature for a series of DHDPE/LLDPE(2) blend samples, as shown in Figure 14. The intense but diffuse scattering is observed in the low scattering angle region only for the blend samples. As already discussed by Stamm[30] and Wignall et al.[31] this diffuse low-angle scattering should originate from the random arrangement of the D and H stems in the lattice. We do not have any additional Bragg peaks in the whole region of scattering angle shown in Figure 14, which should originate from the regular arrangement of the D and H stems. In other words, the WANS data can be also interpreted on the basis of the lattice structure with the D and H chains distributed randomly. In this way all the data obtained in our experiments support the idea of a random arrangement of the chain stems in the lamella of the almost perfectly cocrystallized DHDPE/LLDPE(2) blend system at least. Of course, we may have another possible model which is a compromise between the random reentry model and the regular reentry model.[32] But in this paper we discuss only the relative merits of the two extreme models of the random and regular reentry of the folded chains.

Concluding Remarks

In this paper we have described the SANS data taken for the molten state of the D/H blend samples as a function of temperature and clarified the homogeneous mixing of the D and H chains in the melt. This conclusion is applied to both the cases of DHDPE/LLDPE(2) and DHDPE/LLDPE(3) blend systems. In other words, the difference in the cocrystallization and phase segregation phenomena between these two blend samples does not originate from the difference in the molten state but comes from the crystallization process itself or the crystallization kinetics. As pointed out already, the closeness of the crystallization rate is one of the important factors to govern the cocrystallization of the blend.

By combining all the available data collected so far by ourselves, it has been concluded that the random chain folding mechanism is preferable for the cocrystallized DHDPE/LLDPE(2) blend system, at least. It should be noticed here repeatedly that this blend sample can be cocrystallized almost perfectly even when it is

cooled slowly from the melt. That is to say, the idea of random chain reentry is not limited to the quenched sample but is reasonable also for the sample obtained under the normal crystallization condition. We may naturally speculate that this consideration can be applied also to the normal PE sample.

Acknowledgment. The authors wish to thank Dr. Takeji Hashimoto and Dr. Hirokazu Hasegawa, Faculty of Engineering, Kyoto University, Japan, for their kind permission to use the high-temperature heating cell for the SANS experiment. Grateful acknowledgement is also made to Dr. George D. Wignall, Oak Ridge National Laboratory, for his kind advice and comments in the preparation of the paper.

References and Notes

(1) Tashiro, K.; Stein, R. S.; Hsu, S. L. *Macromolecules* **1992**, *25*, 1801.
(2) Tashiro, K.; Satkowski, M. M.; Stein, R. S.; Li, Y.; Chu, B.; Hsu, S. L. *Macromolecules* **1992**, *25*, 1809.
(3) Tashiro, K.; Izuchi, M.; Kobayashi, M.; Stein, R. S. *Macromolecules* **1994**, *27*, 1221.
(4) Tashiro, K.; Izuchi, M.; Kobayashi, M.; Stein, R. S. *Macromolecules* **1994**, *27*, 1228.
(5) Tashiro, K.; Izuchi, M.; Kobayashi, M.; Stein, R. S. *Macromolecules* **1994**, *27*, 1234.
(6) Tashiro, K.; Izuchi, M.; Kaneuchi, F.; Jin, C.; Kobayashi, M.; Stein, R. S. *Macromolecules* **1994**, *27*, 1240.
(7) Tashiro, K.; Imanishi, K.; Izumi, Y.; Kobayashi, M.; Kobayashi, K.; Satoh, M.; Stein, R. S. *Macromolecules* **1995**, *28*, 8477) (preceding paper in this issue).
(8) Special issue on chain folding problem; *Faraday Discuss. Chem. Soc.* **1979**, *68*.
(9) Brandrup, J.; Immergut, E. H., Eds. *Polymer Handbook*; John Wiley: New York, 1975.
(10) de Gennes, P.-G. *Scaling Concepts in Polymer Physics*; Cornell University Press: Ithaca, NY, 1979.
(11) Balsara, N. P.; Lohse, D. J.; Graessley, W. W.; Krishnamoorti, R. *J. Chem. Phys.* **1994**, *100*, 3905.
(12) Alamo, R. G.; Londono, J. D.; Mandelkern, L.; Stehling, F. C.; Wignall, G. D. *Macromolecules* **1994**, *27*, 411.
(13) Londono, J. D.; Narten, A. H.; Wignall, G. D.; Honnell, K. G.; Hsieh, E. T.; Johnson, T. W.; Bates, F. S. *Macromolecules* **1994**, *27*, 2864.
(14) Sakurai, S.; Hasegawa, H.; Hashimoto, T.; Hargis, I. G.; Aggarwal, S. L.; Han, C. C. *Macromolecules* **1990**, *23*, 451.
(15) Koningsveld, R.; Staverman, A. J. *J. Polym. Sci., A-2* **1968**, *6*, 305.
(16) Koningsveld, R.; Staverman, A. J. *J. Polym. Sci., A-2* **1968**, *6*, 325.
(17) Stockmayer, W. H. *J. Chem. Phys.* **1949**, *17*, 588.
(18) Shibayama, M.; Yang, H.; Stein, R. S.; Han, C. C. *Macromolecules* **1985**, *18*, 2179.
(19) Wignall, G. D.; Londono, J. D.; Lin, J. S.; Alamo, R. G.; Galante, M. J.; Mandelkern, L. *Macromolecules* **1995**, *28*, 3156.
(20) Barham, P. J.; Hill, M. J.; Keller, A.; Rosney, C. C. A. *J. Mater. Sci. Lett.* **1988**, *7*, 1271.
(21) Hill, M. J.; Barham, P. J.; Keller, A.; Rosney, C. C. A. *Polymer* **1991**, *32*, 1384.
(22) Hill, M. J.; Barham, P. J. *Polymer* **1992**, *33*, 4099.
(23) Hill, M. J.; Barham, P. J. *Polymer* **1992**, *33*, 4891.
(24) Hill, M. J.; Barham, P. J.; van Ruiten, J. *Polymer* **1993**, *34*, 4919.
(25) Krishnamoorti, R.; Graessley, W. W.; Balsara, N. P.; Lohse, D. J. *Macromolecules* **1994**, *27*, 3073.
(26) Graessley, W. W.; Krishnamoorti, R.; Reichart, G. C.; Balsara, N. P.; Fetters, L. J.; Lohse, D. J. *Macromolecules* **1995**, *28*, 1260.
(27) Stolken, B.; Ewin, B.; Kobayashi, M.; Nakaoki, T. *J. Polym. Sci., B, Polym. Phys.* **1994**, *32*, 881.
(28) Schelten, J.; Wignall, G. D.; Ballard, D. G. H. *Polymer* **1974**, *15*, 685.
(29) Stamm, F.; Fischer, E. W.; Dettenmaier, M.; Covert, P. *Faraday Disc. Chem. Soc.* **1979**, *68*, 263.
(30) Stamm, M. *J. Polym. Sci., Polym. Phys. Ed.* **1982**, *20*, 235.
(31) Wignall, G. D.; Mandelkern, L.; Edwards, C.; Glotin, M. *J. Polym. Sci., Polym. Phys. Ed.* **1982**, *20*, 245.
(32) Guttman, C. M.; DiMarzio, E. A.; Hoffman, J. D. *Polymer* **1981**, *22*, 597.

MA950415I